The Nonlinear and Ball Pass Effects of a Ball Bearing on Rotor Vibration

D. C. Han*, S. H. Choi, Y. H. Lee** and K. H. Kim*****

(Received June 18, 1997)

A ball bearing is generally assumed as a linear spring in rotor dynamic analysis. In real case, the force equilibrium of the bearing is changed as the relative position of each ball with respect to the direction of radial force. So, the stiffness of the bearing is also changed and is a function of time and position. In this study, the nonlinear characteristics of a ball bearing are considered in analyzing the vibration response of a rotating shaft due to an unbalance force. A finite element method is used to analyze the vibration characteristics of a rotor-bearing system and a direct numerical integration is performed to calculate the transient response of the rotor system. The responses are converted to the frequency domain and the effects of the parametric excitation due to a ball bearing are examined. The test rig for the investigation of the effect of a ball bearing on the rotor vibration is set up and the results are compared with those of numerical calculation. The calculation results show that the amplitudes of the nonlinear model are larger than those of the linear one. The frequencies of the calculations can be matched to the measured frequencies.

Key Words: Ball Bearing, Rotating Shaft, Ball Pass Effect, Nonlinear Spring Model, Super-harmonic Response

Nomenclature

A_1, A_2 : The position of the displaced inner raceway curvature center with respective to the fixed outer raceway curvature center
D : Ball diameter
D_m : Pitch diameter of a bearing
$\{f\}$: Force vector
$\{F\}$: Bearing load vector, $\{F\}^T=\{F_x, F_y, F_z, M_y, M_z\}$
K : Load-deformation factor
l_B : Distance between the inner and the outer raceway curvature center
n : Number of rolling element
$[M], [G], [K]$: Mass, gyroscopic, stiffness matrix
Q : Ball contact load vector, $\{Q\}^T=(Q_x, Q_r)$
r : Radius of curvature of raceway groove
$\{R\Phi\}$: Transformation matrix
$\{u\}$: Inner raceway cross-section displacement vector, $\{u\}^T=(u_x, u_r)$
α : Nominal contact angle
α' : Changed contact angle
δ_c : Contact deformation
$\{\delta\}$: Bearing displacement vector, $\{\delta\}^T=\{\delta_x, \delta_y, \delta_z, \gamma_y, \gamma_z\}$
$\{\Phi\}$: Angular position
ω : Angular velocity of shaft
ω_m : Orbital velocity of rolling element

Subscripts

B : Bearing
i : Inner raceway
o : Outer raceway
x, y, z : x, y, z-axes

*Seoul National University, Professor
**SNU Turbo & Power Machinery Research Center, Senior Researcher
***Samsung Heavy Industries, Research Engineer

: Rolling element index

1. Introduction

For the analysis of rotor systems supported by ball bearings, it is generally sufficient to model the bearing as a linear spring. However, in some modern engineering applications of ball bearings, such as high-speed gas turbines, machine tools, and gyroscopes, the nonlinear characteristics of ball bearings have to be considered carefully to predict vibration characteristics of a rotor-bearing system more accurately. Bearings play an important role in the dynamic behavior of a rotor system. They influence the occurrence of critical speeds, the onset of a dynamic instability, and the magnitude of vibrations of the rotor in response to external forces. Also, bearings may be a source of the external forces for the rotor.

The equation of force equilibrium in a ball bearing is nonlinear and statically indeterminate. So, the load-deformation relationships at the contact point between a rolling element and the raceway have to be considered in the analysis of the load distribution on each ball. This set of nonlinear equations has to be solved by numerical methods, such as Newton-Raphson procedure. In early 1960's, a model to describe the behavior of a ball bearing in a quite general sense is published by A. B. Jones(1960). Jones introduced "race control hypothesis" and analyzed quasi-static characteristics of a ball bearing considering the centrifugal force and the gyroscopic moment yielded by the orbital motion of a rolling element. The flexibility of a shaft and a support structure is also considered and the influence coefficient approach is used. Harris(1991) predicted the friction force and the skidding of a ball based on elasto-hydrodynamic lubrication (EHL) theory and analyzed the motion of the ball. Gupta(1984) derived the dynamic equations of an angular contact ball bearing on the condition of EHL, and analyzed the transient motion of a ball bearing.

Because balls in the bearing are arranged discretely, the relative position of each ball is changing periodically with respect to the direction of the radial load as the shaft rotates. This ball passage through the load line makes the ball bearing stiffness change periodically, as well. This change generates the parametric excitation on a shaft and may be the cause of subharmonic resonance.

In this study, the vibration response due to an unbalance force of a rotating shaft supported by ball bearings is analyzed considering the nonlinear and periodically changing stiffness characteristics of the ball bearing. The bearing stiffness is considered as a nonlinear function of displacement and time in the dynamic equation of the system. The finite element method is used to analyze the rotor-bearing system. The ball bearing stiffness is calculated at each time step considering the variation of internal load distribution due to the ball passage. A direct numerical integration is performed to calculate the unbalance response of the rotor system. The responses are converted to the frequency domain and the effects of the periodic excitation due to the discretely arranged balls are examined. A test rig for the investigation of the effect of a ball bearing on the rotor vibration is set up and the results are compared with those of the numerical calculation.

2. Modeling of a Ball Bearing

Generally, a ball bearing can be modeled such that the outer ring is fixed and the inner ring is displaced from its center by external loads. The force equilibrium contains external loads and contact forces between balls and the inner raceway. Basic ball bearing geometry is shown in Fig. 1.

To simplify the analysis, the following major assumptions are applied(deMul and Vree, 1989).

The structural deformation of the inner and the outer ring of a bearing can be neglected, and only local elastic deformations between the balls and the raceway are considered.

Compared with normal reaction forces between balls and the raceway, the reaction force and the friction between the cage and balls are quite negligible.

The following coordinate systems shown in

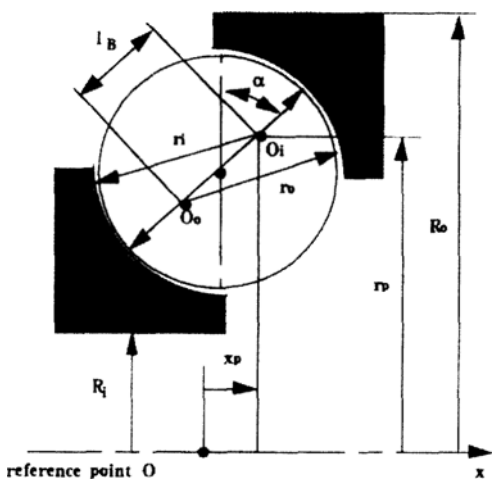

Fig. 1 Ball bearing cross-section geometry.

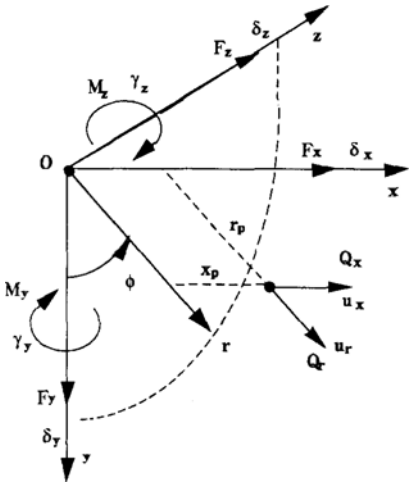

Fig. 2 Bearing Cartesian and cylindrical coordinate systems.

Fig. 2 are chosen for the analysis. A right-handed Cartesian coordinate system x-y-z with the origin O on the inner ring center line defines the direction of an external load vector $\{F\}$ and a bearing displacement vector $\{\delta\}$. x-axis falls on the bearing rotational axis. A cylindrical coordinate system r-Φ-x with the same origin defines the inner raceway cross-section displacement $\{u\}$ and the contact force vector $\{Q\}$ at the angular position Φ of each ball. The center of inner raceway groove curvature is chosen as the inner ring cross-section reference point $\mathrm{Oi}O_i(r_p,\ x_p)$.

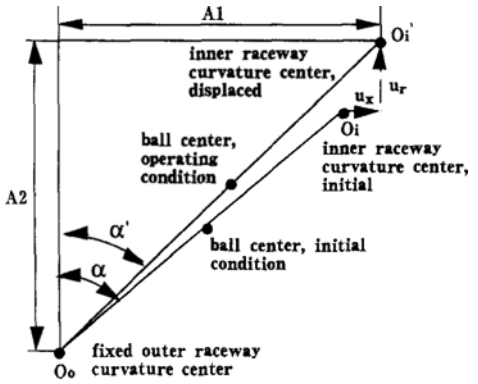

Fig. 3 Positions and displacements of groove centers and ball center in the cross-section i.

If a bearing displacement vector $\{\delta\}$ is given, the inner raceway cross-section displacement $\{u\}$ can be calculated assuming that the displacement $\{\delta\}$ and $\{u\}$ are very small. They can be related linearly as follows;

$$\{u\}=[R\Phi]\cdot\{\delta\} \tag{1}$$

with

$$[R\Phi]=\begin{bmatrix}1 & 0 & 0 & r_p\cos\phi\\ 0 & -\sin\phi & \cos\phi & -x_p\sin\phi\\ & & & r_p\sin\phi\\ & & & -x_p\cos\phi\end{bmatrix} \tag{2}$$

The displacement $\{u\}$ changes the distance between the centers of the inner and the outer raceway curvature and also the magnitude of the contact angle as shown in Fig. 3. A1 and A2 denote the positions of the displaced inner raceway curvature center with respective to the fixed outer raceway curvature center, which is given by

$$\begin{Bmatrix}A_1\\A_2\end{Bmatrix}=\begin{Bmatrix}u_x+l_B\sin\alpha\\u_r+l_B\cos\alpha\end{Bmatrix} \tag{3}$$

where l_B denotes the initial distance between the centers as

$$l_B=r_i+r_o-D \tag{4}$$

The changed contact angle α' is calculated from

$$\tan\alpha'=\frac{A_1}{A_2} \tag{5}$$

The change of the distance between the centers means the contact compression of the ball, which is as follows:

$$\delta_c=\sqrt{A_1^2+A_2^2}-l_B \tag{6}$$

where δ_c denotes the contact deformation.

Classical Herztian contact theory is applied to the analysis of the local deformation between balls and raceway and the ball contact load Q is calculated from

$$Q=K\delta_c^{1.5} \tag{7}$$

where K denotes the load-deformation factor.

The contact force vector is applied along the contact line, which is given by

$$\{Q\}=\begin{Bmatrix}-Q\sin\alpha'\\-Q\cos\alpha'\end{Bmatrix} \tag{8}$$

Using the transformation matrix (2), the contact force $\{Q\}$ is transformed to an equivalent force at the inner ring reference point, and then the sum of the equivalent forces of all balls and the external bearing load $\{F\}$ are in force equilibrium as follos:

$$\{F\}+\sum_{j=1}^{n}[R\Phi]_j^T\cdot\{Q\}_j=\{0\} \tag{9}$$

where index j means the j-th ball.

In practice, the bearing displacements have to be calculated for a given load $\{F\}$. As the set of Eq. (9) is nonlinear for the unknown displacement vector $\{\delta\}$, This equation has to be solved iteratively. Newton-Raphson procedure is applied as follows:

$$\{F\}+\sum_{j=1}^{n}[R\Phi]_j^T\cdot\{Q\}_j+\sum_{j=1}^{n}J(\delta)_j\cdot\{\Delta\delta\}=\{0\} \tag{10}$$

where $J(\delta)_j$, is the jacobian matrix at the j-th rolling element and $\{\Delta\delta\}$ is the change of a solution vector $\{\delta\}$ for the next step in the iteration.

Finally, the Jacobian matrix represents the bearing stiffness matrix,

$$\left[\frac{\partial\{F\}}{\partial\{\delta\}^T}\right]=-\sum_{n=1}^{\infty}J(\delta)_j \tag{11}$$

3. Modeling of a Rotor-Bearing System

For the analysis of rotor vibration, transfer matrix method(TMM) or finite element method (FEM) is generally used. In this paper, FEM is used considering gyroscopic effect, axial force and shear effect.(Nelson, 1980; Ozguven and Ozkon, 1984))

In the analysis of a rotor system supported by ball bearings, these bearings are modeled as linear springs. So, the finite element equation of a typical rotor-bearing system can be written as

$$[M]\{\ddot{X}\}-\omega[G]\{\dot{X}\}+\{[K_B]+[K]\}\{X\}=\{f\} \tag{12}$$

where the stiffness matrices $[K_B]$ of a ball bearing are defined as follows:

$$[K_B]_{lateral}=\begin{bmatrix}K_{yy} & K_{yz}\\K_{zy} & K_{zz}\end{bmatrix}=\begin{bmatrix}\frac{\partial F_y}{\partial\delta_y} & \frac{\partial F_y}{\partial\delta_z}\\\frac{\partial F_z}{\partial\delta_y} & \frac{\partial F_z}{\partial\delta}\end{bmatrix} \tag{13}$$

$$[K_B]_{angular}=\begin{bmatrix}K_{\theta_y\theta_y} & K_{\theta_y\theta_z}\\K_{\theta_z\theta_y} & K_{\theta_z\theta_z}\end{bmatrix}=\begin{bmatrix}\frac{\partial M_y}{\partial\gamma_y} & \frac{\partial M_y}{\partial\gamma_z}\\\frac{\partial M_z}{\partial\gamma_y} & \frac{\partial M_z}{\partial\gamma_z}\end{bmatrix} \tag{14}$$

However, the spring characteristics of a ball bearing are basically nonlinear. And the internal load distribution on the balls varies according to the relative position of each ball with respect to the radial load line(see Fig. 4). So, the bearing stiffness varies periodically. This effect may cause parametric excitations for a rotor. The stiffness variation due to the ball passage through the load line has the frequency as follows:

$$\omega_{ex}=n\cdot\omega_m \tag{15}$$

where n denotes the number of balls and ω_m denotes the ball orbiting speed.

If the slip of the ball motion on the raceway is

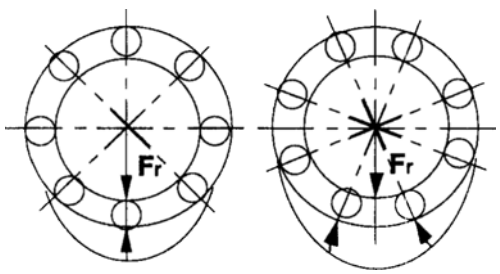

Fig. 4 load distribution of abll bearing.

neglected, m is given by(Harris, 1991)

$$\omega_m=\frac{d_m-D}{2d_m}\omega \tag{16}$$

where d_m is the pitch diameter of a bearing and D is a ball diameter.

So, the reaction forces at the bearing have to be included as a nonlinear function of displacement and time in the equation to analyze the system more accurately. The equations of motion can be rewritten as

$$[M]\{\ddot{X}\}-\omega[G]\{\dot{X}\}+[K]\{X\} =\{L\}-\{f_B(X,\ t)\}\tag{17}$$

where $\{f_B\}$ represents the bearing reaction force vector.

4. Test Rig

The test rig set up for the investigation of the effects of the nonlinear and periodically varied stiffness of a ball bearing on the rotor vibration is shown in Fig. 5. An eccentric mass is located on the rigid disk in the middle of the shaft and the rotating speed of the shaft is 3600 rpm. The deep groove ball bearing, type 6204, is used, of which the basic geometry is given in Table 1. To isolate the motor vibration a flexible coupling is applied effectively.

The acceleration of a bearing housing is measured by an accelerometer and the responses are converted to the frequency domain using an FFT analyzer.

Table 1 Geometry of a 6204 deep groove ball bearing.

Pitch diameter	33.5 mm
Ball diameter	7.938 mm
Inner raceway groove radius	4.01 mm
Outer raceway groove radius	4.20 mm
Ball number	8

5. Results

The load-displacement and the stiffness-displacement relationships for the test bearing are calculated and the results are shown in Fig. 6. The bearing load increases progressively and the

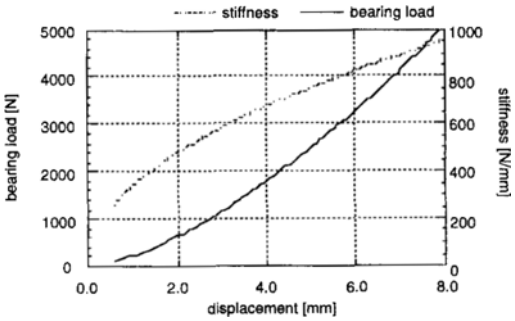

Fig. 6 Load-displacement and stiffness-displacement relationships for a ball bearing, type 6204.

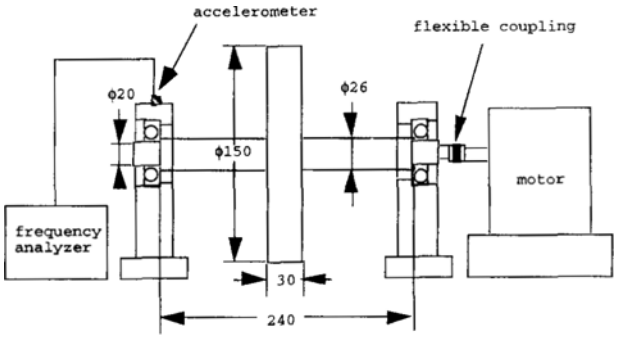

input data
Young's modulus, E : 210 GN/m²
density, ρ : 7850 Kg/m³
bearing : 6204 bearing

Fig. 5 Test rig.

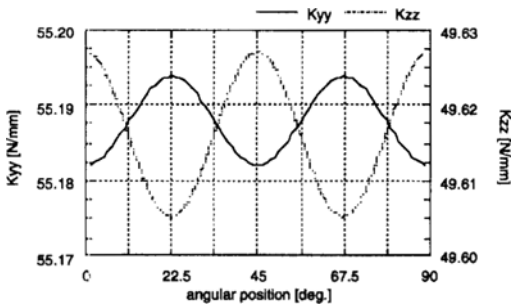

(a)

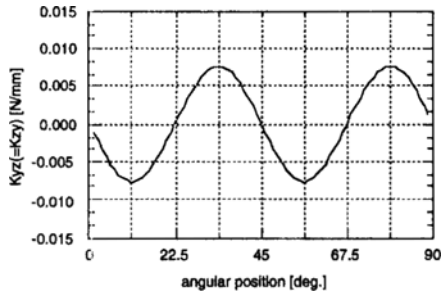

(b)

Fig. 7 Stiffness variation for a ball bearing, type 6204, under a static load.

stiffness increases degressively with the displacements. It is based on the nonlinear characteristics of the contact deformation between balls and the raceway.

The effect of the ball passage on the bearing stiffness under the static load is shown in Fig. 7. The anisotropy of the bearing stiffness is due the difference of the static loads. As the angular position ϕ_1 of a ball with respect to the load line is changed, the bearing stiffness varies periodically. The amplitude of the stiffness variation is relatively small, but would be amplified by the dynamic load due to an unbalance of the rotor.

A finite element model of the test shaft is shown in Fig. 8. Two different models for a ball bearing are applied. They are the linear spring and the nonlinear spring models, which are given in Eqs. (12) and (Bozzi and Anderggent, 1982) respectively. And the direct numerical integration method using implicit -family algorithm(7) is applied to solve the equations. The step size of the time is 0.083 millisecond and the is 0.9. The results of the calculations are shown in Fig. 9 and

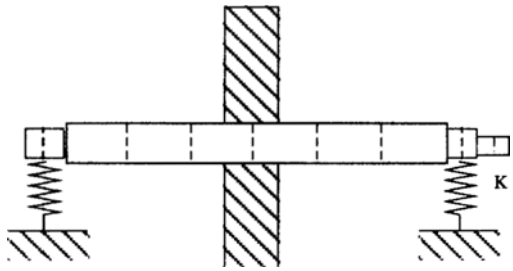

Fig. 8 FEM model of the test rotor.

Table 2. The center of the orbit for the nonlinear spring model is located nearer to the initial bearing center than that for the linear model and the amplitude of the orbit for the nonlinear model is larger than that for the linear model. The reason is that the bearing reaction force and the stiffness increase nonlinearly with the bearing displacements. While the orbit for the linear spring model exhibits only a harmonic response, the orbit for the nonlinear spring model include some superharmonic responses as well as a harmonic response. These vibrations of the rotor are transformed into the frequency domain, as shown in Fig. 10, for the investigation of the superharmonic frequencies. The frequencies showing the peak amplitudes include the rotating frequency, the ball passage frequencies and the sums and the differences of these frequencies.

For the verification of the calculated results the accelerations of the bearing housing, which support the rotating shaft at the speed of 3600 rpm, are measured. Fig. 11(a) shows the power spectrum of the measured acceleration and Fig. 11(b) the frequency spectrum of the calculated reaction force. The peak values appear at 60.0, 123.1, 183.1, 243.1, 246.1, 303.1, 306.1, 366.2, 369.1, 426.3, 429.2, 486.3 and 489.3Hz. The frequency 60.0Hz is the rotating frequency and the frequencies at 183.1, 366.2Hz are due to the excitation frequencies $m\omega_m \pm$, $2n\omega_m - 2\omega$, $n\omega_m + 2\omega$, $2n\omega_m - \omega$, $3n\omega_m - 3\omega$, $2n\omega_m + \omega$, $2n\omega_m - 2\omega$, $2n\omega_m + 2\omega$ and $3n\omega_m - \omega$ between the excitation frequencies by ball passages and rotating speed of shaft are the frequencies at 123.1, 243.1, 246.1, 303.1, 306.1, 369.1, 426.3, 429.2, 486.3 and 489.3Hz, respectively. These frequencies match very well to the frequencies in the power spectrum of the measured

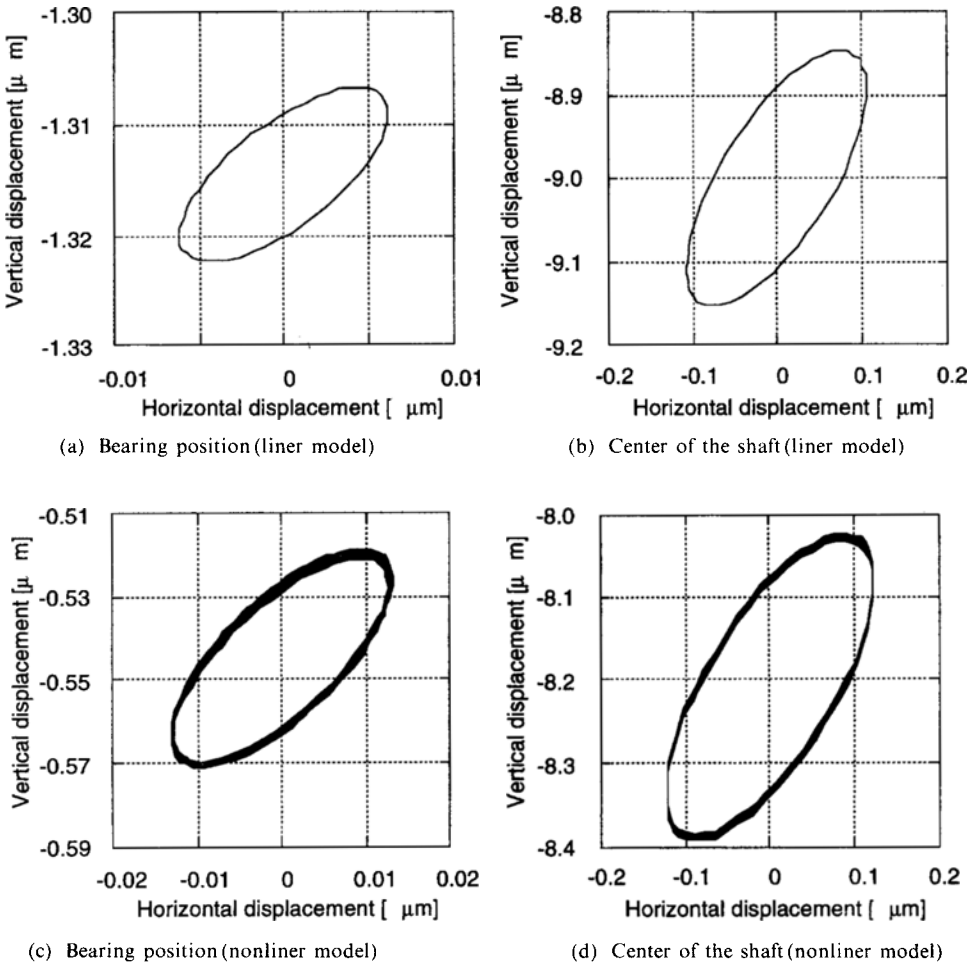

(a) Bearing position (liner model) (b) Center of the shaft (liner model)

(c) Bearing position (nonliner model) (d) Center of the shaft (nonliner model)

Fig. 9 Orbits of the shaft due to the unbalunce force.

Table 2. Numerical results of the two-type models

	Vertical displacement	Amplitude of orbit
Linear spring model	-1.3145E-3	0.923E-5
Nonlinear spring model	-5.4491E-4	0.282E-4

acceleration. The calculated pick values of some high frequencies are smaller than experimental results. It is due to the numerical damping of the numerical integration. The twice frequency of the rotating speed is due to a misalignment or the runout error of a shaft, in general. The frequency of 2ω does not exist in Fig. 11 (b) because those effects are not considered on this study.

6. Conclusions

The vibration response due to an unbalance force of a rotating shaft supported by ball bearings is analyzed considering the nonlinear and periodically varied stiffness.

The stiffness of the ball bearing is calculated with respect to the nonlinear contact deformation and the periodic load distributions on the balls and a finite element method is applied for the rotor dynamic analysis. The periodically varying stiffness is modeled as an external excitation for the rotor-bearing system and the orbital motions of the bearing and the rotor are integrated directly using a ρ-family algorithm.

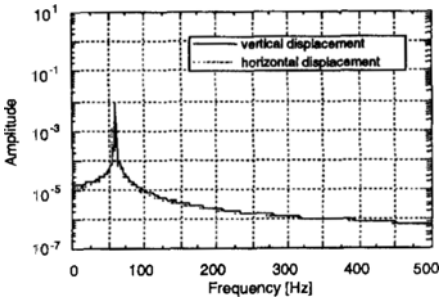

(a) Linear model

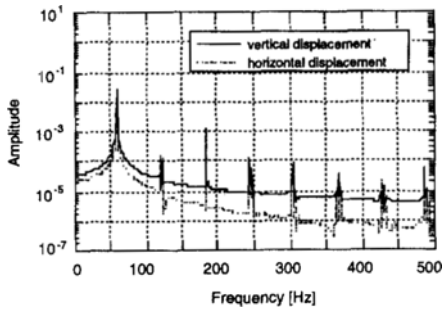

(b) Nonlinear model

Fig. 10 Frequency spectrums of the numerical results (shaft displacements of the bearing position).

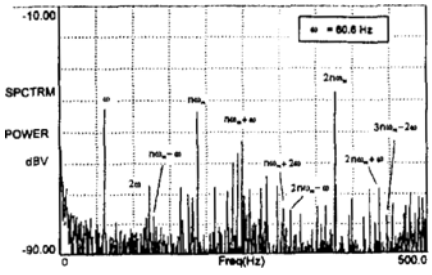

(a) Experimental results measured from the accelometer

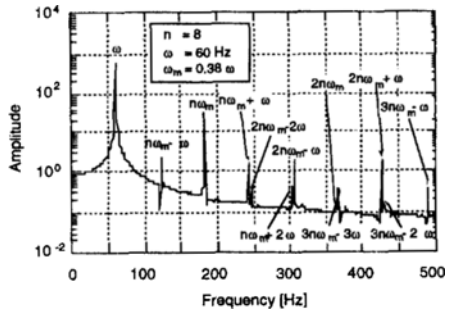

(b) Bearing reaction forces due to the shaft unbalance

Fig. 11 Frequency spectrums of the numerical and experimental results.

The calculated results show that the eccentricity of the orbit for the nonlinear spring model is smaller than that for the linear one and that the amplitude of the orbit for the nonlinear spring model is larger than that for the linear one.

The frequency spectrum of the calculated orbit for the nonlinear model exhibits the peak values at various frequencies including the rotating frequency ω, the excitation frequency $n\omega_m$ by ball passages and the sums and the differences of these frequencies. The power spectrum of the bearing housing acceleration for test rig shows the peak values at all of these frequencies.

It can be concluded that the nonlinear and periodic variation of the stiffness of a ball bearing would be very useful to investigate and predict the harmonic and superharmonic responses of the rotor supported by ball bearings, even though the amplitude of the variation is small enough.

References

Jones, A. B., 1960, "A General Theory for Elastically Constrained Ball and Roller Bearings under Arbitrary Load and Speed Conditions," *ASME Journal of Basic Engineering,* pp. 309 ~320

Harris, T. A., 1991, *Rolling Bearing Analysis,* 3rd ed., Wiley, New york.

Gupta, P. K., 1984, *Advanced Dynamics of Rolling Elements,* Springer-Verlag.

de Mul, J. M., and Vree, J. M., 1989, "Equilibrium and Associated Load Distribution in Ball and Roller Bearings Loaded in Five Degrees of Freedom and while Neglecting Friction-Part 1: General Theory and Application to Ball Bearings," *ASME J. of Tribology,* pp. 142~148

Nelson, H. D., 1980, "A Finite Rotating Shaft Element Using Timoshenko Beam Theory," *ASME J. of Mechanical Design,* Vol. 106, No. 4, pp. 793~803.

Ozguven, H. N. and Ozkan, Z. L., 1984, "Whirl Speeds and Unbalance Response of Multi Bearing Rotors Using Finite Elements,", *J. of Vibration, Acoustics, Stress, and Reliability in Design,* Vol.

106, No. 1, pp. 72~79.

Bazzi, G. and Anderggent, E., 1982, "The ρ-Family of Algorithms for Time-Step Integration with Improved Numerical Dissipation," *Earthquake Eng. and Structural Dynamics,* Vol. 10, pp. 537~550.

M. F. While, 1979, "Rolling Element Bearing Vibration Transfer Characteristics : Effect of Stiffness," *ASME J. of Applied Mechanics,* Vol. 46, pp. 677~684.

Rahnejat, H. and Gohar, R., 1985, "The Vibrations of Radial Ball Bearings," *Proc. Instn. Mech. Engrs.,* Vol. 199, pp. 181~193.